Evaluation of a Coherent Point Drift Algorithm for Breast Image Registration via Surface Markers

Ghazaleh Ahmadian
C. Sean Bohun
Mehran Ebrahimi

Faculty of Science
University of Ontario Institute of Technology (UOIT)
Oshawa, Ontario, Canada

Abstract

Breast Magnetic Resonance Imaging (MRI) is a reliable imaging tool for localization and evaluation of lesions prior to breast conserving surgery (BCS). MR images typically will be used to determine the size and location of the tumours before making the incision in order to minimize the amount of tissue excised.

The arm position and configuration of the breast during and prior to surgery are different and one question is whether it would be possible to match the two configurations. This matching process can potentially be used in development of tools to guide surgeons in the incision process.

Recently, a Thin-Plate-Spline (TPS) algorithm has been proposed to assess the feasibility of breast tissue matching using fiducial surface markers in two different arm positions. The registration algorithm uses the surface markers only and does not employ the image intensities.

In this manuscript, we apply and evaluate a coherent point drift (CPD) algorithm for registration of three-dimensional breast MR images of six patient volunteers. In particular, we evaluate the results of the previous TPS registration technique to the proposed rigid CPD, affine CPD, and deformable CPD registration algorithms on the same patient datasets.

The preliminary results suggest that the CPD deformable registration algorithm is superior in correcting the motion of the breast compared to CPD rigid, affine and TPS registration algorithms.

Keywords: image registration, coherent point drift, breast MRI

1   Introduction

Breast Magnetic Resonance Imaging (MRI) is a reliable imaging tool for localization and evaluation of lesions prior to breast conserving surgery (BCS).

Usually, breast MRI is performed in the prone position, where the breasts are pendant into the imaging coils to overcome motion artifacts from respiration thereby providing high resolution imaging. However in this configuration, the breast shape is different compared to the actual configuration in the operating room table [3]. A goal is to develop a computer assisted surgery (CAS) tool by assigning correspondences between two configurations to recover the transformation that maps one to the other. The results in [3] are based on matching of two configurations, namely *supine arm up* and *supine arm down* positions. Specifically, the scheme applies fiducial surface markers in these two different arm positions that describe the breast surface. The registration algorithm uses the surface markers only and does not employ the image intensities. The aim of the algorithm is to find the correspondence between the markers as well as the transformation that matches one configuration to the other.

Many algorithms exist for rigid and non-rigid alignment of point sets and images [4]. For instance, iterative Closest Point (ICP) algorithm, [2, 9], is one of the most popular methods for rigid point point set registration due to its simplicity and low computational complexity. ICP iteratively assigns correspondences based on a closest distance criterion and finds the least-squares rigid transformation relating the two point sets.

In this paper, we apply a probabilistic method, called the Coherent Point Drift (CPD), introduced by Myronenko et al. [5], for rigid, affine and deformable point set registration on the three-dimensional (3D) breast MRI datasets of six patient volunteers in [3]. We then determine the accuracy of the three CPD registration algorithms and provide a comparison between these and the TPS algorithm [3].

2   Materials and methods

2.1   Data

Table 1 presents the characteristics of patient datasets in [3]. Patient no. 5 was coughing throughout the scanning procedure leading to unacceptably poor quality images in which it was impossible to delineate the tumour; the data from this patient is therefore not included in the study.

Table 1: Characteristics of patient datasets

Patient ID	Matrix size	Field of view (mm^3)	Tumor size arm down (cm^3)	Tumor size arm up (cm^3)
1	$256 \times 256 \times 66$	$180 \times 180 \times 79$	16.8 ± 0.4	18.0 ± 1.1
2	$256 \times 256 \times 56$	$180 \times 180 \times 84$	5.3 ± 0.7	6.9 ± 1.0
3	$256 \times 256 \times 66$	$180 \times 180 \times 79$	80.5 ± 4.1	73.8 ± 1.6
4	$256 \times 256 \times 72$	$180 \times 180 \times 86$	2.4 ± 0.1	2.4 ± 0.4
6	$256 \times 256 \times 46$	$180 \times 180 \times 55$	1.9 ± 0.2	1.5 ± 0.2

2.2   Coherent Point Drift (CPD) registration algorithm

In this section, a brief description of the CPD landmark-based registration is presented. Originally introduced by Myronenko et al. [5] the method begins by constructing an equally weighted Gaussian Mixture Model where D-dimensional centroids are determined by a template point set $Y = (y_1,...,y_M)^T$, a reference point set $X = (x_1,...,x_N)^T$, form the data points and the covariance is taken to be uniform and isotropic. This gives a probability density of $p(x) = \sum_{m=1}^{M} \frac{1}{M} p(x|m)$, where $x|m \sim \mathcal{N}(y_m, \sigma^2 \mathsf{I}_D)$. Note that X and Y can be thought of as $M \times D$ and $N \times D$ matrices. A continuous velocity field v for the template set is defined so that $Y = v(Y_0) + Y_0$ where Y_0 is the set of initial centroid positions. For this implementation, the degree of smoothness of v is characterized by its power spectrum and in particular,

$$\phi(v) = \int_{R^d} \frac{|\tilde{v}(s)|^2}{\tilde{G}(s)} \mathrm{d}s \tag{1}$$

where the over-tilde indicates the Fourier transform and $\tilde{G}$ is a symmetric low-pass filter. In practice, one chooses G to be a Guassian kernal because it is symmetric and positive definite and moreover, $\tilde{G}$ also has a Gaussian form and approaches zero as $\|s\| \to \infty$.

Taking in all these considerations Bayes theorem can be used to find the parameters Y by maximizing the posteriori probability under the prior $p(Y|\lambda) \propto \exp(-\frac{\lambda}{2}\phi(Y))$. Focussing instead of the action of the map v, one is tasked with minimizing the energy function

$$E(\tilde{v}) = -\sum_{n=1}^{N} \log \sum_{m=1}^{M} \exp\left(-\frac{1}{2}\left\|\frac{x_n - y_m}{\sigma}\right\|^2\right) + \frac{\lambda}{2} \int_{R^d} \frac{|\tilde{v}(s)|^2}{\tilde{G}(s)} \mathrm{d}s. \tag{2}$$

The function which minimizes the energy function in above has the form of the radial basis function [6]

$$v(z) = \sum_{m=1}^{M} w_m G(z - y_{0m}). \tag{3}$$

Substituting the solution obtained in (3) back into (2), we obtain

$$E(W) = -\sum_{n=1}^{N} \log \sum_{m=1}^{M} \exp\left(-\frac{1}{2}\left\|\frac{x_n - y_{0m} - \sum_{k=1}^{M} w_k G(y_{0k} - y_{0m})}{\sigma}\right\|^2\right)$$
$$+ \frac{\lambda}{2}\mathrm{tr}(W^T G W) \tag{4}$$

where $G_{M \times M}$ is a square symmetric with elements $g_{ij} = e^{-\frac{1}{2}\|\frac{y_{0i} - y_{0j}}{\beta}\|^2}$ and $W_{M \times D} = (w_1,...,w_M)^T$ is a matrix of the Gaussian kernel weights. For details on optimizing $E(W)$, please refer to [6].

The matching procedure required a set of parameters. We manually tuned the parameters (Table 2) for the algorithm to yield satisfactory matching of the markers in the volunteer dataset. For a detailed description of each parameter see [5].

Table 2: The CPD algorithm parameters

Symbol	Definition	Number
N	number of effective eigenvectors	40
β	width of Gaussian distribution	3
λ	regularization weight	28
w	noise weight	0.1
fgt	Fast Gauss Transform	2
corresp	compute correspondence vector at the end of registration	300
tol	tolerance	1e-6

"There are three free parameters in the method: α, β, σ. Parameter α represents the trade-off between data fitting and smoothness regularization. Parameter β reflects the strength of interaction between points. The value of σ serves as a capture range for each Gaussian mixture component. Deterministic annealing for σ is used, starting with a large value σ and gradually reducing it according to $\sigma = \alpha\sigma$, where σ is annealing rate (normally between $[0.92 0.98]$), so that the annealing process is slow enough for the algorithm to be robust. The gradual reducing of σ leads to a coarse-to-fine matching strategy" [5].

2.3 Marker selection and matching

The position of the MR-visible markers in the two arm-up and arm-down images for each patient were semi-manually selected and computed using a GUI tool that was developed in house [3]. The CPD registration [5] was then employed to match the markers for rigid, affine, and deformable transformations.

2.4 Tumor segmentation

Three independent observers, all of whom were experienced in looking at breast MR images, segmented the tumours of each of the patients using TurtleSeg (Interactive 3D Image Segmentation Software) [7] that provides a semi-manual tool for segmentation [3].

"Here, we present data for five of the patients from the study named as patient $1, 2, 3, 4,$ and 6 and the number of markers which we use for arm up, arm down positions in all of 5 patient datasets are 34 and 33, respectively. The tumour of patient no. 3 could not be reliably identified and segmented even with the help of a radiologist therefore we segmented an enhancing cyst that was clearly visible in the images instead. Also, the attachment of the surface marker has caused a local distortion of the skin surface for patient no. 4" [3].

3 Result

We computed the Dice measure of overlap between the tumour in the reference and the registered arm up images presented in Table 3. In addition, we computed the Centre of Mass (COM) of the tumours and evaluated the Euclidean distance between the tumours in the reference and arm up images; this is defined as the COM-displacement Table 4.

The focus of this study is the matching of supine breast datasets which were acquired with two different arm positions using the CPD algorithm and the positions of surface markers. Our goal was to localize the tumour using the described scheme. We used manual segmentations of the lesions to assess the Dice overlap and COM-displacement metrics.

Based on the results presented in Tables 3 and 4, it can be recognized that the deformable CPD point sets registration Dice scores were generally superior than the CPD rigid and affine except in patient 4 and 6. It can be observed that Dice measure of patient 4 was not consistent with the other patients in Table 3. These could be due to several factors. The initial unregistered arm-up and down positions have a displacement of 46 mm which is the largest among all of the patients in the study. Also, due to a miscommunication problem in placing the markers, only one side of the breast was covered by the markers for patient 6 " [3]. In addition, the tumour is close to the COM of the markers and as expected CPD

rigid gave the best results compared to CPD deformable, affine and TPS for patient 6. As we expected, the result of the experiments vary based on the tumour size, shape, and location.
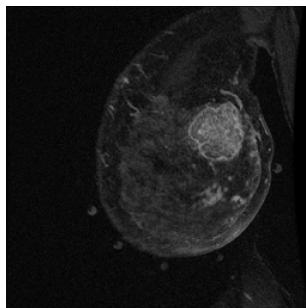
Table 3 evaluates the Dice measures of tumour overlap, and Table 4 indicates COM-displacement of tumours in millimeters before and after registration. Three values in each cell represent the values calculated based on each of the three independent tumour segmentations. The maximum possible number of available matched markers have been used for each patient. In Figure 1, the result of the 3 different registration schemes for the first patient can be observed.
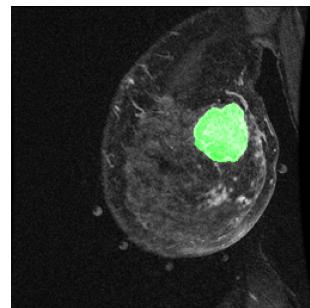
Table 3: Dice score(%)

Patient ID	Unregistered	TPS registered	CPD-rigid registered	CPD-affine registered	CPD-deformable registered
1	(A) 28 (B) 24 (C) 20	(A) 77 (B) 79 (C) 74	(A) 65 (B) 67 (C) 64	(A) 76 (B) 81 (C) 76	(A) 78 (B) 83 (C) 79
2	(A) 0 (B) 0 (C) 0	(A) 75 (B) 63 (C) 57	(A) 60 (B) 53 (C) 52	(A) 72 (B) 60 (C) 59	(A) 75 (B) 64 (C) 64
3	(A) 26 (B) 23 (C) 28	(A) 75 (B) 74 (C) 77	(A) 79 (B) 79 (C) 79	(A) 75 (B) 73 (C) 76	(A) 85 (B) 84 (C) 83
4	(A) 0 (B) 0 (C) 0	(A) 20 (B) 23 (C) 21	(A) 0 (B) 0 (C) 0	(A) 20 (B) 19 (C) 25	(A) 0 (B) 0 (C) 0
6	(A) 6 (B) 10 (C) 6	(A) 61 (B) 59 (C) 59	(A) 81 (B) 81 (C) 79	(A) 70 (B) 69 (C) 70	(A) 72 (B) 71 (C) 73

Table 4: COM-displacement (mm)

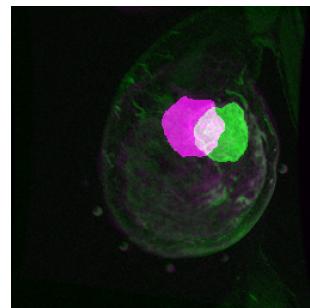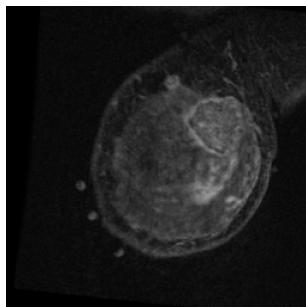| Patient ID	Unregistered	TPS registered	CPD-rigid registered	CPD-affine registered	CPD-deformable registered
1	(A) 17.5 (B) 18.5 (C) 19.5	(A) 2.7 (B) 3.0 (C) 4.0	(A) 6.5 (B) 6.5 (C) 7.4	(A) 3.2 (B) 3.1 (C) 4.1	(A) 2.5 (B) 2.5 (C) 3.6
2	(A) 33.0 (B) 33.1 (C) 32.0	(A) 0.9 (B) 1.5 (C) 2.2	(A) 6.2 (B) 7.3 (C) 7.3	(A) 2.8 (B) 2.8 (C) 2.4	(A) 3.1 (B) 3.6 (C) 2.5
3	(A) 31.6 (B) 32.2 (C) 30.3	(A) 9.0 (B) 9.3 (C) 7.9	(A) 4.7 (B) 4.8 (C) 4.5	(A) 9.8 (B) 10.3 (C) 9.0	(A) 4.0 (B) 4.1 (C) 4.2
4	(A) 46.8 (B) 46.7 (C) 46.1	(A) 8.5 (B) 8.3 (C) 8.5	(A) 21.0 (B) 23.7 (C) 21.0	(A) 10.6 (B) 10.2 (C) 10.0	(A) 17.6 (B) 19.6 (C) 17.7
6	(A) 11.0 (B) 10.9 (C) 11.2	(A) 3.9 (B) 4.2 (C) 5.2	(A) 1.2 (B) 1.2 (C) 3.4	(A) 2.8 (B) 3.0 (C) 2.3	(A) 2.5 (B) 2.6 (C) 2.4

(a) Reference (arm parallel)
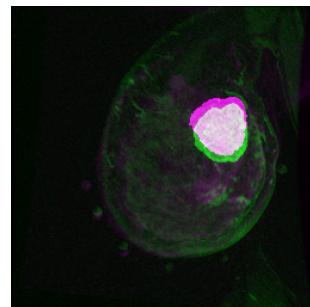

(b) Segmented tumour in reference
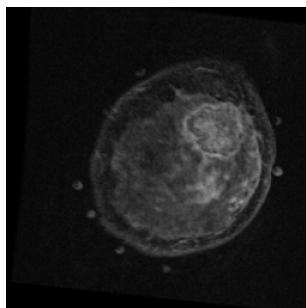

(c) Template (arm up)

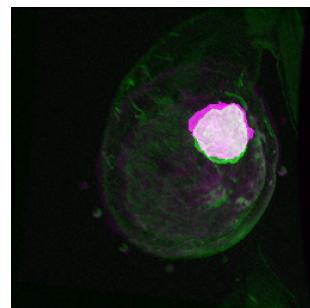*(d)* Template overlay on reference

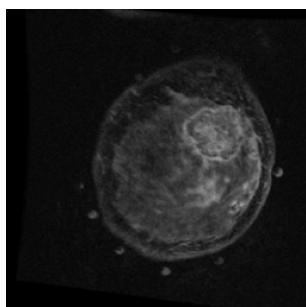*(e)* Rigid registered template

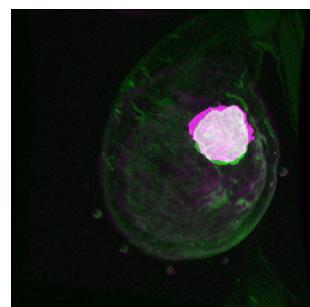*(f)* Rigid registered overlay

(g) Affine registered template

(h) Affine registered overlay

(i) Deformable registered template

(j) Deformable registered overlay

Fig. 1: The CPD registration for patient 1; Slice 34 of the 3D volume is shown.

4 Conclusion

The experimental results suggest that the deformable CPD registration of 3D breast MRI can perform more accurately compared to the rigid, affine and TPS registration methods. In general, the motion of the breast is nonrigid so that rigid or affine transformations are not sufficient enough to describe the motion. These prelimi-nary results also demonstrate that in general the experiments are affected by the tumour size, shape, and location.

The CPD registration results reported in this paper took 0.4 to 0.6 seconds of CPU time on a standard PC running Matlab, which is significantly lower than the computation time using TPS (under a minute) reported in [3] .

In order to further assess the feasibility of the registration approach in a surgical setting, more volunteer patient datasets with tumours will be required.

Acknowledgments

References

[1] Beatty, J David and Porter, Bruce A, Contrast-enhanced breast magnetic resonance imaging: the surgical perspective, The American journal of surgery, 193, 5, 600–605, (2007), Elsevier.

[2] Besl, Paul J. and McKay, Neil D., Method for registration of 3-D shapes, Proc. SPIE, 1611, 586-606, (1992), 10.1117/12.57955, http://dx.doi.org/10.1117/12.57955.

[3] Ebrahimi, Mehran and Siegler, Peter and Modhafar, Amen and Holloway, Claire MB and Plewes, Donald B and Martel, Anne L, Physics in medicine and biology, 59, 7, 1589, (2014), IOP Publishing

[4] Modersitzki, Jan, FAIR: flexible algorithms for image registration, 6, (2009),SIAM.

[5] Myronenko, Andriy and Song, Xubo, Point set registration: Coherent point drift, IEEE transactions on pattern analysis and machine intelligence, 32, 12, 2262–2275, (2010), IEEE.

[6] Myronenko, Andriy, Xubo Song, and Miguel A. Carreira-Perpinán, Non-rigid point set registration: Coherent point drift, Advances in Neural Information Processing Systems, 1009–1016, (2006).

[7] Top, Andrew and Hamarneh, Ghassan and Abugharbieh, Rafeef, Active learning for interactive 3D image segmentation, International Conference on Medical Image Computing and Computer-Assisted Intervention, 603–610, (2010), Springer.

[8] Wahba, Grace, Spline models for observational data, 59, (1990), SIAM.

[9] Zhang, Zhengyou, Iterative point matching for registration of free-form curves and surfaces, 13, 2, 119–152, (1994), Springer.